Negative heat capacity of sodium clusters

Juan A. Reyes-Nava, Ignacio L. Garzón, and Karo Michaelian
Instituto de Física, Universidad Nacional Autónoma de México, Apartado Postal 20-364, 01000 México Distrito Federal, México
(Received 26 July 2002; published 1 April 2003)

Heat capacities of Na_N, $N=13$, 20, 55, 135, 142, and 147, clusters have been investigated using a many-body Gupta potential and microcanonical molecular-dynamics simulations. Negative heat capacities around the cluster meltinglike transition have been obtained for $N=135$, 142, and 147, but the smaller clusters ($N=13$, 20, and 55) do not show this peculiarity. By performing a survey of the cluster potential-energy landscape (PEL), it is found that the width of the distribution function of the kinetic energy and the spread of the distribution of potential-energy minima (isomers) are useful features to determine the different behavior of the heat capacity as a function of the cluster size. The effect of the range of the interatomic forces is studied by comparing the heat capacities of the Na_{55} and Cd_{55} clusters. It is shown that by decreasing the range of the many-body interaction, the distribution of isomers characterizing the PEL is modified appropriately to generate a negative heat capacity in the Cd_{55} cluster.

DOI: 10.1103/PhysRevB.67.165401 PACS number(s): 36.40.Ei, 64.70.Dv

I. INTRODUCTION

Negative microcanonical heat capacity in atomic and molecular clusters was theoretically predicted by considering simple models of the distribution of local minima that characterize the potential-energy landscape (PEL) of clusters.[1] In that study, it was found that for high values of the parameter involving the ratios of the vibrational frequencies corresponding to the global and local isomers, the caloric curve displays an *S*-shaped loop, with a negative heat capacity in the vicinity of the melting point.[1] In another study on the solid-liquid transition of clusters,[2] it was shown that in microcanonical simulations of Lennard-Jones clusters, an increase in total energy causes a temperature reduction. This effect was related to the broadening of the cluster kinetic-energy distribution toward lower-energy values.[2]

Although the existence of negative heat capacity in physical systems such as stars or star clusters,[3,4] and in fragmenting nuclei[5,6] is well known, this peculiar effect gained a lot of interest in the field of atomic and molecular clusters due to recent experimental results where a negative heat capacity was measured for a 147-atom sodium cluster.[7] In this study, the photofragmentation mass spectra were used to measure the internal energy of free, mass selected clusters with known temperature. These measurements were used to determine the microcanonical caloric curve of the Na_{147}^+ that shows the characteristic *S*-shaped (backbending) feature, indicating a negative heat capacity.[7] The negative value of the microcanonical heat capacity was interpreted by considering that a finite system upon melting tries to avoid partly molten states and prefers to convert some of its kinetic energy into potential energy.[7,8] This peculiarity has been attributed to the nonadditivity of the total energy of a cluster with finite size.[7,8]

Microcanonical heat capacities of metal clusters have been theoretically investigated using constant-energy molecular dynamics (MD) with many-body potentials[9–11] and an orbital-free version of the first-principles MD method.[12,13] In these studies, heat capacities of fcc transition and noble-metal clusters with up to 23 atoms were calculated to characterize their meltinglike transition.[9] In another study, on the melting of sodium clusters,[10] the microcanonical caloric curve of the Na_{55} cluster was obtained. However, in not one of these studies was a signature of a negative heat capacity found. Similar results, indicating the nonexistence of a negative heat capacity in constant-energy orbital-free first-principles MD simulations of larger sodium clusters (Na_{55}, Na_{92}, and Na_{142}), were obtained.[13] Nevertheless, in such calculations the simulation time employed was too short to obtain converged results.[13] On the other hand, in microcanonical MD simulations of Al_N, $N=7$, 13, 55, and 147, clusters, a negative heat capacity was obtained for the larger Al_{147} cluster.[11]

In the present work, motivated by the availability of experimental techniques that allow the measurement of the microcanonical heat capacity and other thermal properties of mass selected metal clusters,[14–16] we theoretically investigate the behavior of the heat capacity of sodium clusters in the size range of 13–147 atoms. In our approach, constant-energy MD simulations are performed using a phenomenological many-body potential that mimics the metallic bonding of sodium clusters. This approximation allows us to use simulation times of the order of ~ 50 ns, in order to obtain converged averages of the microcanonical heat capacity and other cluster thermal properties. Our main objective is to gain additional insights into the conditions that determine if a cluster has a negative heat capacity. The main finding of this work shows that the width of the distribution function of the kinetic energy and the spread of the distribution of the potential-energy minima (isomers), characterizing the PEL, are useful features to determine the signature of the cluster heat capacity. In Sec. II, we provide the theoretical background on which this study is based. The results and their discussion are given in Sec. III, and Sec. IV contains a summary and the conclusions of this work.

II. THEORETICAL BACKGROUND

The heat capacity and temperature of sodium clusters as a function of the cluster total energy are calculated through

constant-energy MD simulations using the microcanonical expressions derived in Refs. 17 and 18:

$$\frac{C}{Nk_B}=\left[N-N\left(1-\frac{2}{3N-6}\right)\langle K\rangle\langle K^{-1}\rangle\right]^{-1}, \quad (1)$$

$$T=\frac{2\langle K\rangle}{(3N-6)k_B}, \quad (2)$$

where K is the kinetic energy of the cluster, k_B is the Boltzmann constant, and $\langle\cdots\rangle$ denotes a time average. In these formulas, $3N$ was changed to $3N-6$, the number of degrees of freedom of the system, since the calculations are performed for a nontranslating and nonrotating cluster in a three-dimensional space (the position of the center of mass was fixed and the total momentum was held to zero during the simulations).

In our implementation of the constant-energy MD method, the Newton's equations of motion are solved with the Verlet algorithm[19] using a time step of 2.4 fs, which provides total-energy conservation within 0.001%. A typical calculation consists in heating up a cluster from its lowest-energy solidlike configuration until it transforms into a liquidlike cluster. To simulate this procedure the cluster total energy is increased in a steplike manner by scaling up the atomic velocities. For each initial condition the cluster was equilibrated during 10^4 time steps and the time averages of the physical quantities are calculated using 10^7 time steps. This averaging time is increased by a factor of 2 when the cluster is in the region of the solid-to-liquid transition in order to ensure the calculation of fully converged averages.

To model the metallic bonding in sodium clusters we used the many-body Gupta potential,[20] which is based on the second moment approximation of a tight-binding hamiltonian.[21] Its analytical expression is given by

$$V=\sum_{i=1}^{N} V_i, \quad (3)$$

$$V_i=A\sum_{j\neq i} e^{-p(r_{ij}/r_0-1)}-\xi\left(\sum_{j\neq i} e^{-2q(r_{ij}/r_0-1)}\right)^{1/2}, \quad (4)$$

where r_0, A, ξ, p, and q are adjustable parameters.[21] For sodium clusters, these parameters have been fitted to band-structure calculations.[22] Their values are $A=0.015\,95$ eV, $\xi=0.291\,13$ eV, $r_0=6.99$ bohr, $p=10.13$, and $q=1.30$.[22] This phenomenological many-body potential has been used to study the meltinglike transition in sodium clusters of different sizes using Monte Carlo[10] (MC) and constant-energy MD simulations.[23] A good qualitative agreement has been obtained between structural and thermal properties calculated using the Gupta potential[10,23] and those generated from first-principles methods.[12,13] An additional advantage in using this potential is that it allows simulation times of the order of 50 ns, necessary to obtain fully converged time averages in the meltinglike transition region.

III. RESULTS AND DISCUSSION

The microcanonical heat capacities of the Na_N, $N=13$, 20, 55, 135, 142, and 147, clusters, calculated using Eq. (1), are displayed in Fig. 1. For $N=13$, 20, and 55, they are continuous functions of the cluster total energy showing a maximum value that is characteristic of a meltinglike transition.[10,12,13,23] On the other hand, the heat capacity of the larger clusters ($N=135$, 142, and 147) shows two discontinuity points and a continuous negative-valued interval between them. This peculiar behavior in the heat capacity is related with a backbending loop in the caloric curve (temperature as a function of the total energy).[1,2,24,25] In fact, our calculated microcanonical caloric curves of Na_{135}, Na_{142}, and Na_{147} show the backbending loop at the same energies where the heat capacity takes negative values (see the caloric curves shown in Fig. 2 of Ref. 23). In previous studies, the negative slope (backbending loop) of the microcanonical caloric curve has been attributed to a peculiar behavior of the cluster entropy as a function of energy that shows a *dent* with inverted curvature in the region of the solid-liquid transition.[1,2,7,8,25]

In the present work, we analyze the behavior of the microcanonical heat capacity of sodium clusters from a different perspective. First, we consider Eq. (1) and obtain the condition to have a negative value in the heat capacity:

$$Z_E\equiv\langle K\rangle\langle K^{-1}\rangle>\frac{3N-6}{3N-8}. \quad (5)$$

Figure 2 displays the values of Z_E (black dots) as a function of the cluster total energy E, which were calculated from a time average using the MD trajectories. In the same scale the threshold value $Z_c\equiv(3N-6)/(3N-8)$ for each cluster size is given. In Fig. 2, it can be graphically seen how the relative difference between Z_E and Z_c changes with the cluster size. For the three smaller clusters [see panels (a)–(c) in Fig. 2], the Z_E values do not overcome the threshold value, whereas for the three larger clusters there is a range of total energy where Z_E satisfies the condition to have negative heat capacities [see panels (d)–(f) in Fig. 2].

In order to investigate what determines a negative value of the heat capacity, we consider the quantity Z_E. This is the product of the averages of the kinetic energy and of the inverse of this quantity, and therefore, its value will depend on the distribution function of the kinetic energy, $g_E(K)$. The average of any function of the kinetic energy $f(K)$ can be obtained through the following expression:

$$\langle f_E\rangle_g=\int f(K)g_E(K)dK. \quad (6)$$

Since the distribution function of the kinetic energy, $g_E(K)$, determines the behavior of Z_E, it is useful to analyze $g_E(K)$ at different values of the cluster total energy E. The calculation of this quantity is straightforward from the constant-energy MD simulations. Figure 3 shows g_E as a function of the normalized mean deviation $\delta K=(K-\langle K\rangle)/\langle K\rangle$ for three different energies, corresponding to the cases where the cluster is in the solidlike and liquidlike phases, and at the middle

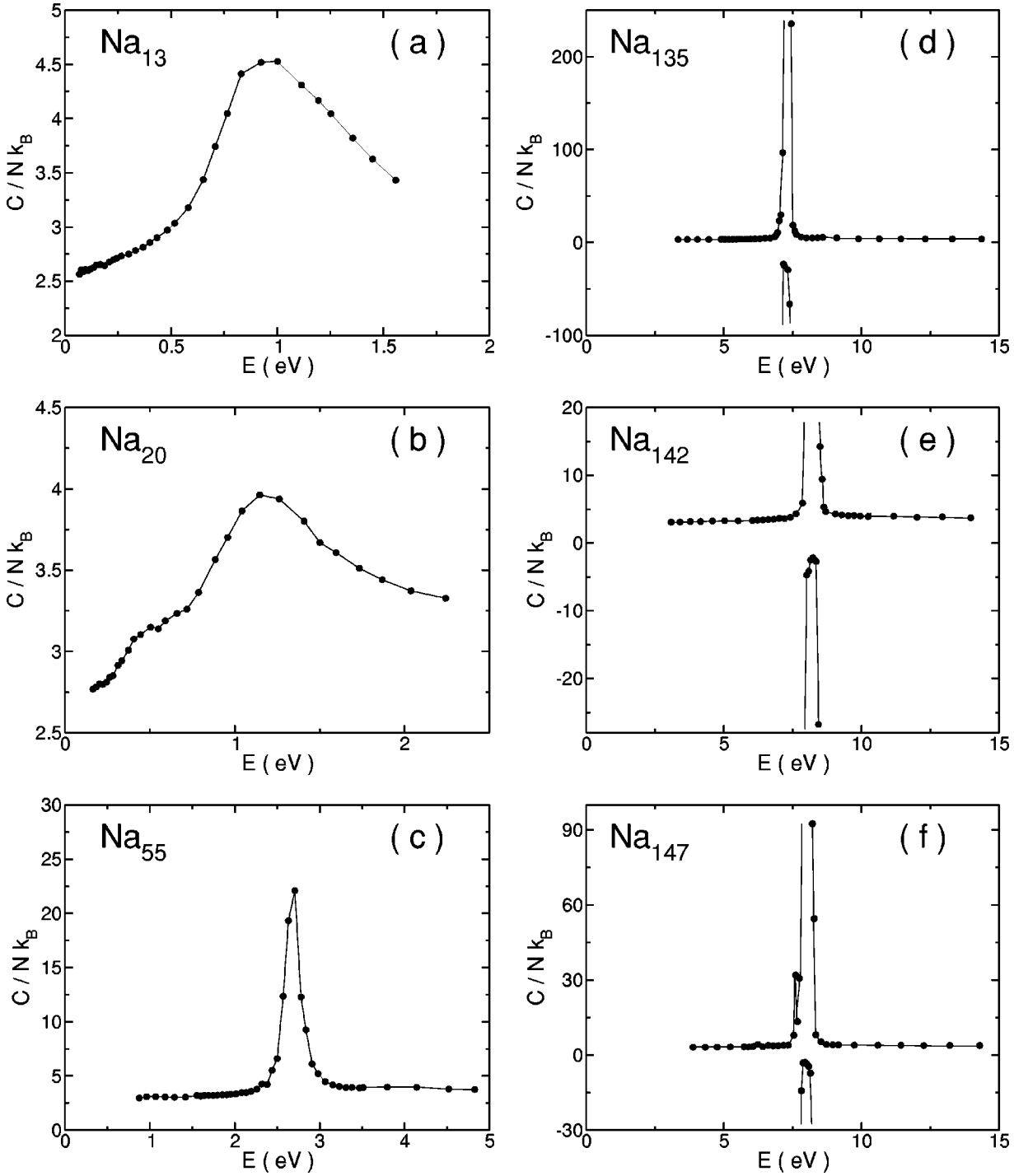

FIG. 1. Heat capacity of Na_N, $N=13$ (a); 20 (b); 55 (c); 135 (d); 142 (e); and 147 (f) clusters. The cluster energy is calculated taking as reference the value of the binding energy of the most-stable (lowest-energy) configuration given in Table I of Ref. 23.

of the meltinglike transition. The analysis of g_E as a function of δK, instead of K, has the advantage that it allows the comparison, on the same scale, of the line shapes of this function at different cluster energies and for different cluster sizes.

As a general trend, it is found that g_E becomes narrower for increasing cluster sizes, indicating a larger relative dispersion of the kinetic-energy values for the smaller clusters. This result is expected since it confirms the increment of fluctuations in kinetic energy of a physical system that decreases in size. A common characteristic of g_E, existing in the six clusters investigated, is the larger broadening of the distribution function when the cluster is at the meltinglike transition. At lower (solidlike phase) and higher (liquidlike phase) energies, the width of g_E is smaller, whereas at the phase transition the fluctuations in kinetic energy, as expected, should increase.

For the three smaller clusters which do not have negative

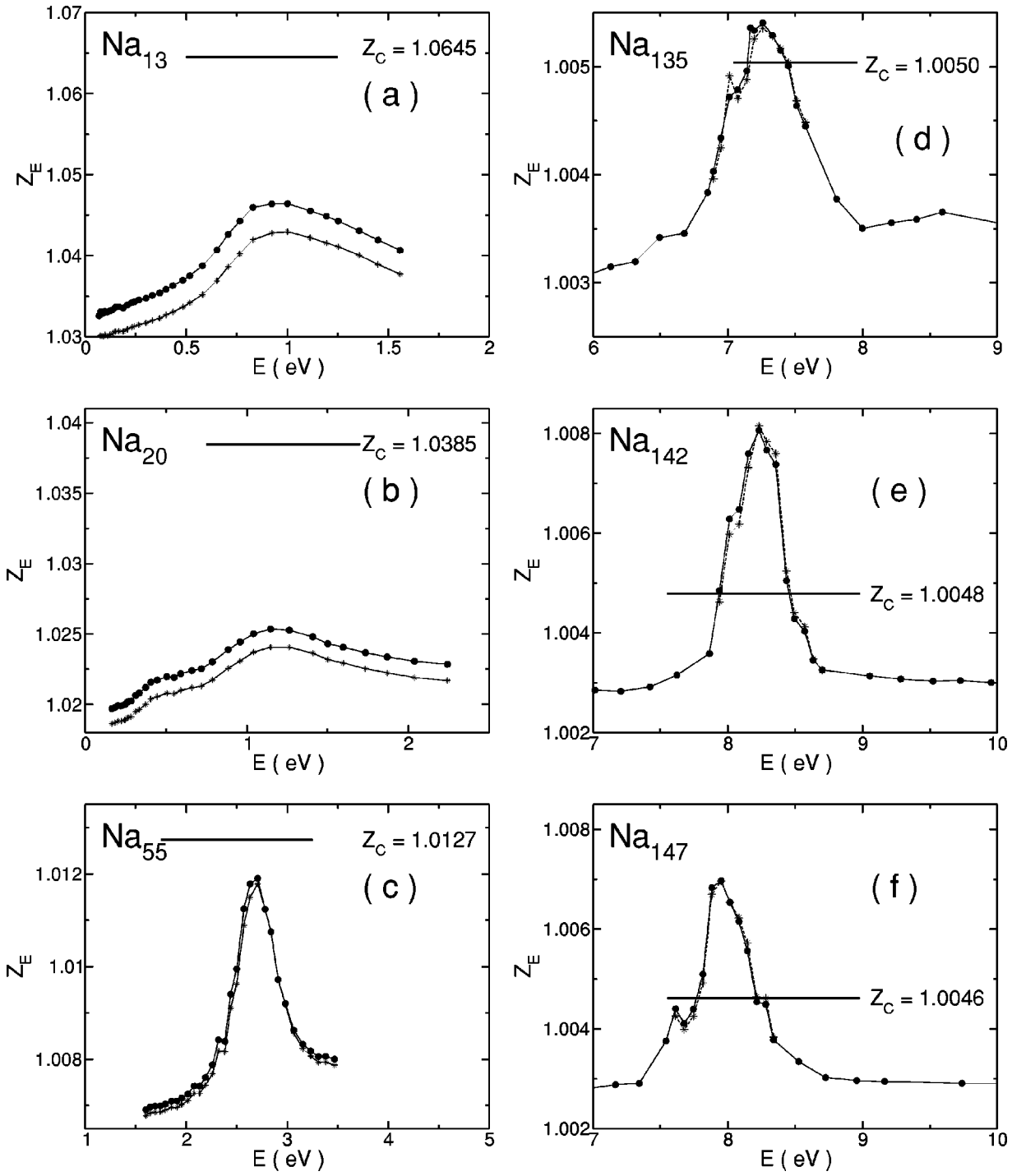

FIG. 2. Energy dependence of the Z_E (black dots) and $Z_E^{(2)}$ (stars) values for Na_N, $N=13$ (a); 20 (b); 55 (c); 135 (d); 142 (e); and 147 (f) clusters. The Z_E values were calculated using Eq. (5) whereas the $Z_E^{(2)}$ values, which are an approximation of Z_E according to Eq. (9), were obtained using the second moment of the distribution function of the kinetic energy. See the related text for an explanation of the difference between these quantities. The cluster energy is calculated taking as reference the value of the binding energy of the most-stable (lowest-energy) configuration given in Table I of Ref. 23.

heat capacity, $g_E(\delta K)$ shows a nearly symmetric line shape independent of the cluster energy [see panels (a)–(c) of Fig. 3]. In contrast, Na_{142} and Na_{147}, which show a negative heat capacity, have a distribution function $g_E(\delta K)$ with a shoulder towards positive values of δK, at energies in the middle of the melting region [see panels (e) and (f) of Fig. 3]. Although this difference in the distribution function of the kinetic energy could be a useful feature to determine the existence of a negative heat capacity, the Na_{135} cluster would be an exception to this rule since its $g_E(\delta K)$ does not show a resolved shoulder in its line shape [see panel (d) in Fig. 3], but it has a negative heat capacity.

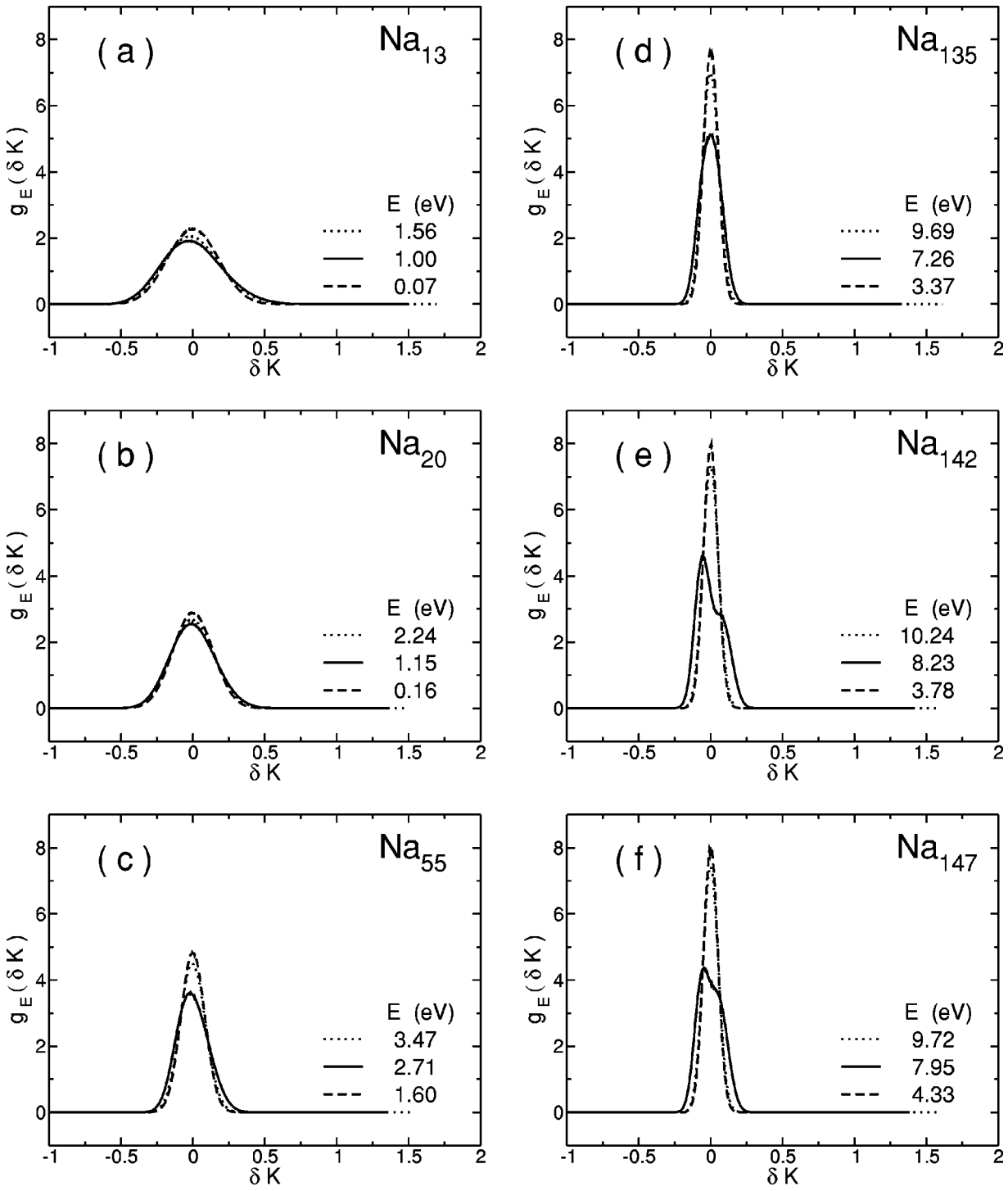

FIG. 3. Distribution function of the kinetic energy for Na_N, $N=13$ (a); 20 (b); 55 (c); 135 (d); 142 (e); and 147 (f) clusters. The three curves displayed in each panel correspond to the solidlike (lower-energy), meltinglike (intermediate energy), and liquidlike (higher-energy) phases.

On the other hand, a characteristic of g_E that would be useful to determine the sign of the heat capacity is the width of the distribution function, which can be obtained through its second moment:

$$\langle(\delta K)^2\rangle_g = \int (\delta K)^2 g_E(\delta K) d(\delta K). \tag{7}$$

The second moment of g_E corresponds to the second term in the expansion of Z_E, which can be obtained from the left-hand term of Eq. (5):[17,18]

$$Z_E = 1 + \langle(\delta K)^2\rangle_g + \cdots. \tag{8}$$

By taking terms up to second order in this expansion, assuming that $\langle \delta K\rangle_g \ll 1$, Z_E can be approximated by

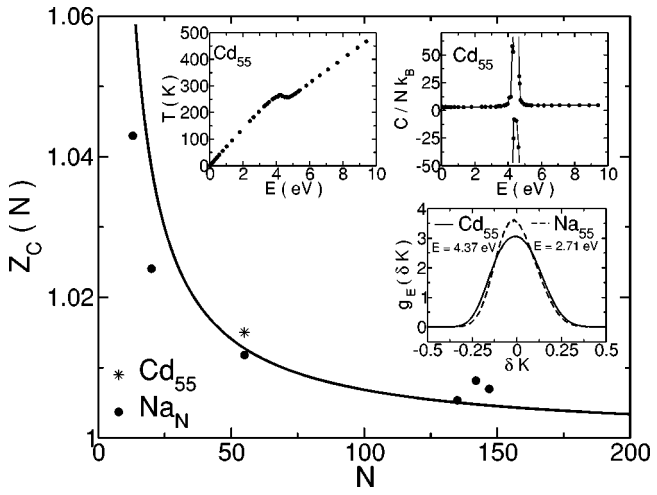

FIG. 4. Comparison of the maximum values of $Z_E^{(2)}$ (black dots for the Na_N clusters) and the threshold Z_c (continuous line) as a function of the cluster size. The star shows the maximum value of $Z_E^{(2)}$ for the Cd_{55} cluster. The upper insets show the energy dependence of the caloric curve and the heat capacity of the Cd_{55} cluster. The inset at the low right corner shows the g_E as a function of the normalized mean deviation of the kinetic energy of the Cd_{55} cluster, and its comparison with Na_{55}, calculated at $E=4.37$ eV and $E=2.71$ eV, respectively.

$$Z_E \approx Z_E^{(2)} = 1 + \langle (\delta K)^2 \rangle_g . \tag{9}$$

Since the $Z_E^{(2)}$ values can be calculated using g_E and Eq. (7), it is possible to check the validity of this approximation, which can only be applied to systems with a finite number of particles. Figure 2 shows the values of $Z_E^{(2)}$ (stars) as a function of the cluster energy. It can be seen that the difference with Z_E is small for the three smaller clusters and negligible for the three larger ones. Then, $Z_E^{(2)}$ can be considered as a quantitative measure of the width (second moment) of the distribution function of the kinetic energy, and can be used to determine the sign of the heat capacity. Figure 4 shows the maximum values of $Z_E^{(2)}$ (black dots) calculated for energies at the middle of the melting transition, and their comparison with the threshold values Z_c as a function of the cluster size (full line). From this figure, it is obvious that although the width of g_E is relatively large for the three smaller clusters, the corresponding maximum values of $Z_E^{(2)}$ are below the threshold Z_c, and therefore these clusters do not show a negative heat capacity. On the other hand, the width of g_E for Na_{135}, Na_{142}, and Na_{147} is smaller than for Na_{13}, Na_{20}, and Na_{55}, however, Z_c is a faster decreasing function of the cluster size N, such that the maximum of $Z_E^{(2)}$ lies above the threshold values, indicating that the larger clusters have negative heat capacities. Then, the above results suggest that the width of the distribution function of the kinetic energy is a useful property to determine the sign of the heat capacity of clusters. However, this quantity not only depends on the cluster size, but also on the characteristics of the PEL.

To illustrate the importance of the topology of the PEL, we have investigated the behavior of the heat capacity of 55-atom clusters using the many-body Gupta potential,[20] shown in Eqs. (3) and (4), for the different metals listed in Tables I and III of Ref. 21, and in Table II of Ref. 22. Our results show that the Cd_{55} cluster (with the following parameter values:[21] $A=0.0416$ eV, $\xi=0.4720$ eV, $p=13.639$, and $q=3.908$) has a negative heat capacity, but none of the other 55-atom clusters show this peculiarity. The upper insets of Fig. 4 show the calculated caloric curve with the corresponding backbending loop and the heat capacity with negative values for a range of total-energy values of the Cd_{55} cluster. The inset at the lower right corner of Fig. 4 shows g_E as a function of the normalized mean deviation of the kinetic energy for both, the Na_{55} and Cd_{55}, clusters. It can be seen that the broadening of g_E is larger in Cd_{55} than in Na_{55} such that it generates a maximum value of $Z_E^{(2)}$ (this value corresponds to the point represented by a star in Fig. 4) that overcomes the threshold Z_c, and consequently, the Cd_{55} cluster displays a negative heat capacity. This comparison with the Na_{55} cluster that does not show this peculiarity indicates that although both clusters have the same size, their dynamical properties defined by their corresponding PEL's generate different behavior in their heat capacities.

In order to investigate the influence of the PEL on the different widths of the distribution function of the kinetic energy of the Na_{55} and Cd_{55} clusters, further studies are necessary. In this direction, the calculation of short-time averages of the kinetic energy and periodic quenchings of instantaneous configurations during the MD trajectories allow us to obtain the distribution of potential-energy minima (isomers) that are accessible at different cluster energies.[24] Figure 5 displays the normalized distribution of potential-energy minima, obtained by periodical quenchings using MD trajectories at a total energy where the cluster is at the middle of the melting transition, for the Na_{55} and Cd_{55} clusters. It can be noticed that the number of isomers with higher energy relative to the global minimum are larger for the Cd_{55} cluster in comparison with the results obtained for Na_{55}. This result can be explained by taking into account that the range of the interatomic forces is shorter in Cd than in Na clusters, mainly due to the higher value of the q parameter in the many-body Gupta potential.[26] The physical reason for the larger number of minima at short range is the loss of accessible configuration space as the potential wells become narrower, thus producing barriers where there are none at long range.[27]

To show how the distribution of potential-energy minima determines the broadening of the distribution function of the kinetic energy, we approximate the complex topology of the PEL by a set of independent harmonic potential wells in the $3N-6$ dimensional space. Each one of these wells is associated to the different potential-energy minima forming the distribution of isomers shown in Fig. 5. For each potential-energy minimum denoted by l, the distribution function of the kinetic energy at a total energy E, in the harmonic approximation, is given by[2,17]

$$g_{E,l}(K) = C_l (E - \Delta_l - K)^{(3N-7)/2} K^{(3N-7)/2}, \tag{10}$$

where Δ_l is the potential energy of the isomer l, relative to the potential-energy value of the lowest-energy isomer, and C_l is a normalization constant such that

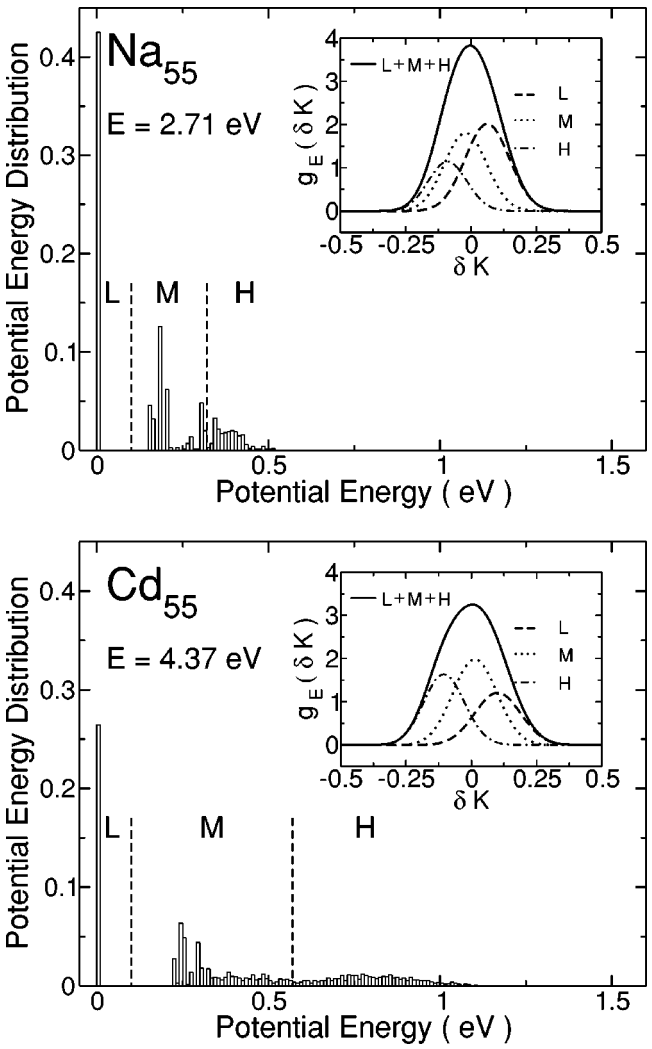

FIG. 5. Normalized distribution of potential-energy minima for the Na_{55} and Cd_{55} clusters. This distribution was obtained from 2000 quenchings separated by 10 000 time steps during a MD trajectory of 20×10^6 time steps. The values of $E=4.37$ eV (Cd_{55}) and $E=2.71$ eV (Na_{55}) correspond to the cluster energies when they are at the middle of the meltinglike transition. The vertical dashed lines separate intervals of low (L), medium (M), and high (H) potential energy. The insets show the total (full line), including the L, M, and H intervals, and partial (taking different subsets of isomers) $g_{E,har}$, as a function of the normalized mean kinetic energy.

$$\int_0^{E-\Delta_l} g_{E,l}(K)dK=1. \tag{11}$$

The distribution function of the kinetic energy $g_{E,har}$, at a total energy E, corresponding to the whole PEL can be constructed by adding up the contribution of each harmonic potential well, weighted by the probability, $\omega_{E,l}$, of finding a given isomer during the quenching from the MD trajectories. This probability is given by the height of the distribution shown in Fig. 5. Then, $g_{E,har}$ is given by

$$g_{E,har}=\sum_{l=1}^{l_{max}} \omega_{E,l} g_{E,l}(K), \tag{12}$$

with

$$\sum_{l=1}^{l_{max}} \omega_{E,l}=1. \tag{13}$$

By using the data from the whole distribution of isomers in Fig. 5, the distribution function of the kinetic energy $g_{E,har}$ was calculated for the Cd_{55} and Na_{55} clusters. They are displayed in the insets of Fig. 5 (full lines). A comparison between $g_{E,har}$ and the exact g_E (obtained from the MD simulation and displayed in the lower right inset of Fig. 4) shows that there is a good agreement between the two distribution functions. This indicates that g_E is determined mainly from the number of isomers and the probability to find them (height of the distribution), rather than from other features of the PEL such as saddle points. The advantage in introducing $g_{E,har}$ in this discussion is related with the fact that it is possible to analyze the broadening of this distribution function of the kinetic energy by considering different subsets of potential-energy minima (isomers). This is useful to determine what regions of the PEL are more relevant to increase the width of $g_{E,har}$, and investigate the appearance of the negative heat capacity. The insets of Fig. 5 show three partial distribution functions $g_{E,har}$, considering different subsets of isomers corresponding to three intervals of low (L), medium (M), and high (H) potential-energy values. By analyzing the relative contribution of these subsets to the width of $g_{E,har}$ for the Cd_{55} and Na_{55} clusters, it is found that the larger broadening in the cadmium cluster is mainly due to the larger contribution of the isomers in the range of high potential energy which are spreaded along a larger interval than those corresponding to the Na_{55} cluster. The width of $g_{E,har}$ for the Na_{55} cluster is smaller, since there are proportionally less isomers with high potential energy and they are extended over a shorter interval of values. As was mentioned above, the physical reason for this difference in the distribution of isomers between the Cd_{55} and Na_{55} clusters is the shorter range of the many-body forces existing in the cadmium cluster as compared with those present in the sodium cluster. A similar result was obtained for 55-atom clusters using a pairwise Morse potential for different values of the range of the interatomic forces.[27] In that case the backbending loop in the caloric curve (negative heat capacity) was obtained using a Morse potential with a range of the interatomic forces that is shorter than the range characteristic of alkali metals that have long-ranged interactions.[27]

Therefore, if a detailed characterization of the distribution of isomers forming the PEL of clusters is performed, the broadening of g_E may be estimated, and by the comparison of the corresponding $Z_E^{(2)}$ and Z_c values, it would be possible to predict the sign of the heat capacity of clusters.

IV. SUMMARY

The microcanonical heat capacity of sodium clusters has been calculated using constant-energy MD simulations and the many-body Gupta potential. Negative values for the heat capacity at energies where the cluster is at the meltinglike transition were found for Na_{135}, Na_{142}, and Na_{147}. The

smaller sodium clusters Na_N, $N=13$, 20, and 55, do not show this peculiarity. An analysis of the calculated distribution function of the kinetic energy g_E for the six clusters investigated shows that the width of this distribution function is a useful feature to determine the sign of the heat capacity. It was found that although the broadening of g_E is larger for the smaller clusters, it is not enough to overcome the corresponding threshold value to obtain a negative heat capacity. However, since this threshold is a fast decreasing function of the cluster size, the broadening of g_E in the larger clusters is enough to generate a negative heat capacity.

It was also shown that the broadening of g_E depends on the distribution of potential-energy minima that characterize the PEL of clusters. Specifically, as the range of the many-body interactions is decreased (like in the case of Cd clusters), the number of local minima with higher energy increases generating a larger broadening in g_E, and consequently a negative heat capacity. The analysis presented in this paper shows how the complex topology of the PEL can be explored to extract the main features that determine the sign of the heat capacity of metal clusters.

ACKNOWLEDGMENTS

This work was supported by Conacyt-Mexico under Project No. G32723-E and DGAPA-UNAM under Project IN104402. J.A.R.-N. acknowledges financial support from DGEP-UNAM.

[1] M. Bixon and J. Jortner, J. Chem. Phys. **91**, 1631 (1989).
[2] P. Labastie and R.L. Whetten, Phys. Rev. Lett. **65**, 1567 (1990).
[3] W. Thirring, Z. Phys. **235**, 339 (1970).
[4] D. Lynden-Bell, Physica A **263**, 293 (1999).
[5] D.H.E. Gross, Rep. Prog. Phys. **53**, 605 (1990).
[6] M. D'Agostino *et al.*, Phys. Lett. B **473**, 219 (2000).
[7] M. Schmidt, R. Kusche, T. Hippler, J. Donges, W. Kronmüller, B. von Issendorff, and H. Haberland, Phys. Rev. Lett. **86**, 1191 (2001).
[8] M. Schmidt and H. Haberland, C. R. Phys. **3**, 327 (2002).
[9] J. García-Rodeja, C. Rey, L.J. Gallego, and J.A. Alonso, Phys. Rev. B **49**, 8495 (1994).
[10] F. Calvo and F. Spiegelman, J. Chem. Phys. **112**, 2888 (2000).
[11] J. Jellinek and A. Goldberg, J. Chem. Phys. **113**, 2570 (2000).
[12] A. Aguado, J.M. López, J.A. Alonso, and M.J. Stott, J. Chem. Phys. **111**, 6026 (1999).
[13] A. Aguado, J.M. López, J.A. Alonso, and M.J. Stott, J. Phys. Chem. B **105**, 2386 (2001).
[14] M. Schmidt, R. Kusche, W. Kronmüller, B. von Issendorff, and H. Haberland, Phys. Rev. Lett. **79**, 99 (1997).
[15] M. Schmidt, R. Kusche, B. von Issendorff, and H. Haberland, Nature (London) **393**, 238 (1998).
[16] R. Kusche, T. Hippler, M. Schmidt, B. von Issendorff, and H. Haberland, Eur. Phys. J. D **9**, 1 (1999).
[17] E.M. Pearson, T. Halicioglu, and W.A. Tiller, Phys. Rev. A **32**, 3030 (1985).
[18] S. Sawada and S. Sugano, Z. Phys. D: At., Mol. Clusters **14**, 247 (1989).
[19] L. Verlet, Phys. Rev. **159**, 98 (1967).
[20] R.P. Gupta, Phys. Rev. B **23**, 6265 (1981).
[21] F. Cleri and V. Rosato, Phys. Rev. B **48**, 22 (1993).
[22] Y. Li, E. Blaisten-Barojas, and D.A. Papaconstantopoulos, Phys. Rev. B **57**, 15 519 (1998).
[23] J.A. Reyes-Nava, I.L. Garzón, M.R. Beltrán, and K. Michaelian, http://arxiv.org/abs/physics/0207068, Rev. Mex. Fis. **48**, 450 (2002).
[24] D.J. Wales, Mol. Phys. **78**, 151 (1993).
[25] D.J. Wales and R.S. Berry, Phys. Rev. Lett. **73**, 2875 (1994).
[26] K. Michaelian, M.R. Beltrán, and I.L. Garzón, Phys. Rev. B **65**, 041403(R) (2002).
[27] J.P.K. Doye and D.J. Wales, J. Phys. B **29**, 4859 (1996).